applied sciences

MDPI

Article

Integration of Micro-Structured Photovoltaic Cells into the Ultra-Light Wing Structure for Extended Range Unmanned Aerial Vehicles

Octavian Narcis Ionescu [1,2,*], Ileana Cernica [2], Elena Manea [2], Catalin Parvulescu [2], Alin Istrate [3], Gabriela Ionescu [1] and Mirela Petruta Suchea [2,4,*]

[1] Faculty of Electrical and Mechanical Engineering, Petroleum and Gas University of Ploiesti, 100680 Ploiesti, Romania; ionescu_g_ro@yahoo.com
[2] National Institute for Research and Development in Microtechnologies (IMT-Bucharest), 023573 Bucharest, Romania; Ileana.cernica@imt.ro (I.C.); elena.manea@imt.ro (E.M.); catalin.parvulescu@imt.ro (C.P.)
[3] Autonomous Flight Technology Ltd., 24042 Bucharest, Romania; alin.istrate@aft.ro
[4] Center of Materials Technology and Photonics, School of Engineering, Hellenic Mediterranean University, 71410 Heraklion, Greece
* Correspondence: octavian.ionescu@imt.ro (O.N.I.); mira.suchea@imt.ro or mirasuchea@hmu.gr (M.P.S.)

Abstract: There have been large developments in the unmanned aerial vehicles (UAV) industry over the last decade. Although UAV development was mainly for military related use in the beginning and despite there being fear surrounding the release of this technology to the open market for quite a long time, nowadays, there are a variety of applications where UAVs are used extensively, such as in agriculture, infrastructure inspection and monitoring, mobile retranslation relays for communications, etc. One of the weaknesses of electrically propelled UAVs is flight autonomy; there is often a difficult trade-of between the weight of the payload, batteries, and surface to be surveyed that is necessary to determine. There have been many attempts to use photovoltaic cells to increase the flight time for UAVs; however, a reliable solution has not yet been developed. The present paper presents improvements that have been conducted to extend the autonomy of electrically derived UAVs: instead of gluing photovoltaic cells on the wings, the new approach embeds the solar cells into the wing structure as well as develops a new wing that is significantly lighter to compensate for the weight added by the photovoltaic cells. It was demonstrated that by using this approach, a 33% increase in the flight time can be achieved with only one modified wing in a prototype vehicle.

Keywords: photovoltaic integration; microstructures; ultra-light wing; UAV

check for updates

Citation: Ionescu, O.N.; Cernica, I.; Manea, E.; Parvulescu, C.; Istrate, A.; Ionescu, G.; Suchea, M.P. Integration of Micro-Structured Photovoltaic Cells into the Ultra-Light Wing Structure for Extended Range Unmanned Aerial Vehicles. *Appl. Sci.* **2021**, *11*, 10890. https://doi.org/10.3390/app112210890

Academic Editor: Antonio Di Bartolomeo

Received: 26 October 2021
Accepted: 15 November 2021
Published: 18 November 2021

Publisher's Note: MDPI stays neutral with regard to jurisdictional claims in published maps and institutional affiliations.

Copyright: © 2021 by the authors. Licensee MDPI, Basel, Switzerland. This article is an open access article distributed under the terms and conditions of the Creative Commons Attribution (CC BY) license (https://creativecommons.org/licenses/by/4.0/).

1. Introduction

Nowadays, at the international level [1], statistics show that by the end of 2025, there will be over 20,000,000 operational drones/UAVs, with an estimated value of transactions in this field of over USD 45.8 billion. Within these types of UAVs, the ones with applications relating to social security represent over 60%; consequently, drones are expected to have a high market potential. The crisis of personnel working in agriculture as well as the development of many large farms that cover thousands of hectares are pushing farmers and agricultural associations to use UAVs with increased autonomy for surveillance and culture monitoring. The development of highly advanced video-cameras as well as artificial intelligence is also a factor that helps in the development of UAVs.

One of the most convenient methods to extend the autonomy of electrically propelled UAVs is to install photovoltaic cells on the wings and/or fuselage and to use the electrical power generated by these cells to charge the batteries. There have been numerous attempts to install photovoltaic cells on UAV wings [2–5]. The main issues that have been encountered in all of these attempts are generated by the efficiency and the reliability of the

photovoltaic cells. The attempt to use large-sized photovoltaic cells was hindered by wing vibrations of the UAVs, which led to silica wafer cracking and sometimes the disruption of soldered connections. Moreover, due to the frequency at which UAVs manoeuvre, the solar irradiation is not equally dispersed on the cell surface, leading to a less efficient conversion. Another disrupting factor was that the weight of the solar cell matrix, the material used to connect them, and the resin used to glue them on the wings increased significantly the weight of the UAV, thus decreasing the weight of the usable payloads.

The approach presented here was completely different and was oriented in two main directions:

- To develop an ultra-light UAV wing;
- To develop photovoltaic cells that are suitable to be embedded into the structure of the wing.

These two efforts are interconnected by specific requirements such as the mechano-climatic loads that are specific for fixed wings.

The present paper is structured into two main parts: A part consisting of an introduction as well as discussion of the design and fabrication processes, and the second part presents the tests and the prototype validation, conclusions, and perspectives. A short video is also included in the Supporting Materials that documents the flight of the prototype.

2. Design and Fabrication

In order to shorten the development process, the design of the ultra-light UAV wing was based on the aerodynamic shape developed for Hirus, an operational UAV from the industrial partner involved in this work. The initial wing structure of Hirus was based on glass fibre fabric embedded into an epoxy resin. In the original design, two composite layers of fibre glass fabric were placed over a layer of aerogel (Rohacell-Evonik Industries AG, Essen, Germany). To compensate for the PV and the addition weight of the wiring, instead of fibre glass fabric, which has a relatively high weight, it was decided that a new composite material based on carbon fibre (Vuhlets®, Texpack® S.r.l. Via Galileo Galilei, 24 25030 Adro (BS) Italy) with a lower weight (40 g/m^2) and higher resistance would be used. Thus, the initial mass of the wing, which was around 850 g when made of glass fibre, was decreased to 550 g, providing 300 g of additional weight for the photovoltaic cells and wires. Figure 1 presents a schematic transversal section through the UAV's wing, which presents a detailed sandwich structure: carbon fibre fabric, aerogel, carbon fibre fabric.

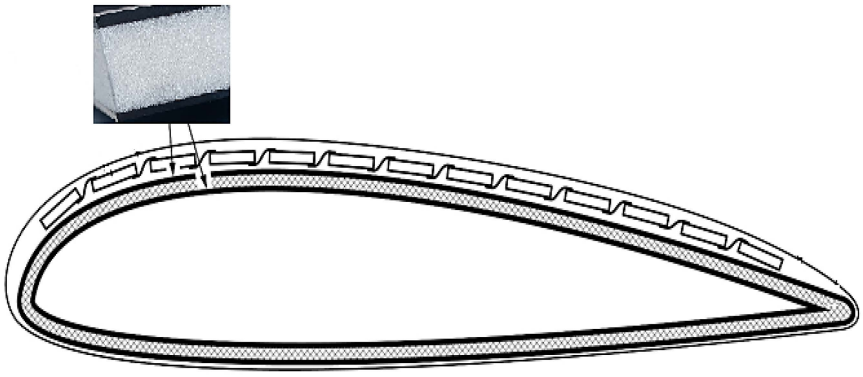


Figure 1. Transversal section through the wing with detailed sandwich structure: carbon fibre fabric, aerogel, carbon fibre fabric.

The next step was to establish the best dimensions and technology for photovoltaic cell fabrication. For this step a thorough calculation of efforts and wing bending was conducted.

A simplified evaluation of the deformations according to the pressure difference applied on the surface of the photovoltaic element (using average values at ambient temperature [6]) was performed using the calculation theory used at bars on the two main directions of the photovoltaic element (length, width).

The following values were used to verify the determinations that were made and to estimate (coarsely) the maximum deformations of the wing on the two directions due to the pressure that was on it during the flight:

- L = 20 mm, length of the element;
- d = 10 mm, width of the element;
- g = 0.3 mm, element thickness;
- E = 160 GPa, silicon modulus of elasticity (for semiconductors) [7].

The formula used for simulating the wing bending was [1]

$$y(x) = \frac{w}{24 \cdot E \cdot I} \cdot \left(x^4 - 2 \cdot D \cdot x^3 + D^3 \cdot x \right).$$

where:

- $y(x)$ represents the deformation of the bar as a function of the position x along the bar;
- w represents the load evenly distributed along the bar;
- E is the mode of elasticity;
- I is the moment of inertia of the section;
- x is the position along the bar;
- and D is the length of the bar.

Figure 2 presents a graphic representation of the UAV's wing deformation on the two axes.

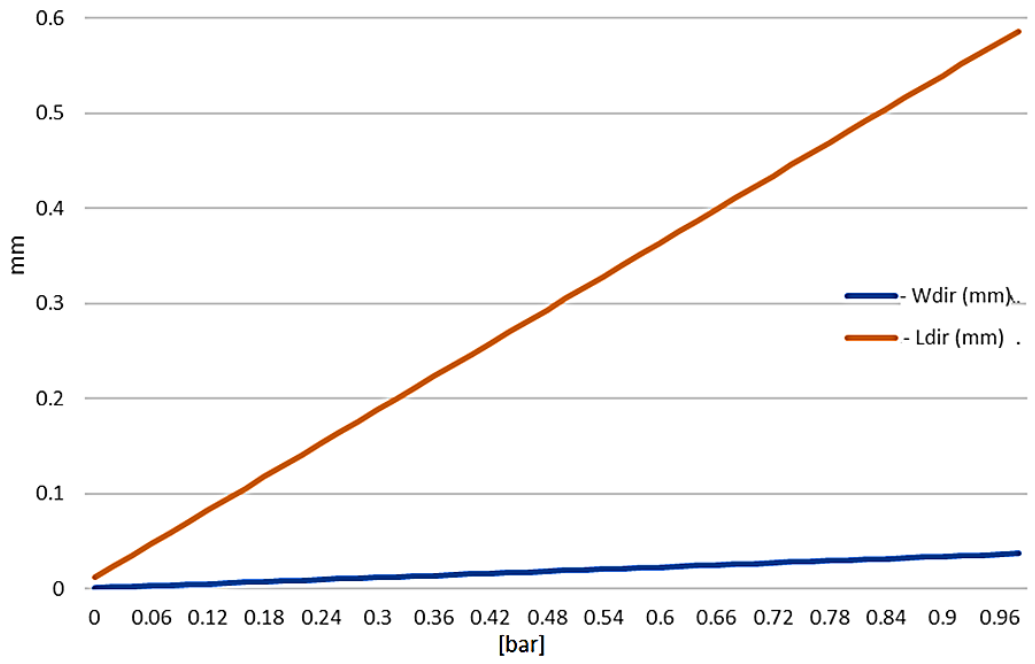


Figure 2. UAV's wing deformation on the two axes.

As one can observe, Figure 2 shows the progressive load simulated using the fixed-bar principle to be applied on the wing in order to establish the bending amplitude (on both sides L—length, and d—wide). It can be observed that the maximum deformation of the wing on the length (L) at a pressure of 1 atm lies below 0.6 mm. For a bar supported at the ends and that is uniformly loaded, the maximum deformation (maximum arrow) occurs at half the distance between the ends. (For a wing that is up to 1.5 m wide and with UAV

speeds of up to 250 km/h, it was determined that the dimensions of the photovoltaic cells should be L = 20 mm, d = 10 mm.)

In order to verify the maximum allowable deformation of the photovoltaic cells, destructive tests were also performed using the MECMESIN MultiTest 2.5 Software-controlled force test system (Newton House, Spring Copse Business Park, Slinfold, West Susssex, United Kingdom), the results of which will be presented further on in Section 3. Following the practical tests, a maximum deformation arrow of 0.8 mm was found to be acceptable in the "L" direction, which is part of the calculation of the maximum deformation of the wing.

The photovoltaic structures were made of silicon wafers with a diameter of 3 inches, an orientation <100>, type p, resistivity 1–3 Ω·cm, and a thickness of 350 μm. The size of the solar cell structures with a textured surface is 10×22 mm^2 (the connexion ribbon/front pad/collector was extended from 1 mm to 2 mm in order to provide a larger connection surface). The texturing of the cell surfaces was conducted through a photolithographic process that defined inverse pyramids with sides of 10 μm that were placed in a network between the collection contacts/electrodes of the photocarriers generated by incident light.

By taking into consideration the wing profile as it is presented in Figure 1 that presents a significant curvature, it was obvious that not all of the photovoltaic cells will have the same exposure to the incident Sun light. In order to overcome this disadvantage, it was decided to improve the design of the cells to obtain a much better exposure to the irradiation source. It was determined that the solution that would be used would be to texturize the surface of the cells and thus reduce reflection losses and increase absorption in the near IR spectral range [8]. The total absorption on the textured incident surface increased by 4 times compared to that of the flat surface.

One problem specific problem that was encountered during materials selection was the establishment of the right type of epoxy resin to be used for embedding the photovoltaic cells into the wing structure. It is well known that some resins change their optical properties (transparency) if exposed to ultraviolet rays or heat. These tests were conducted on a representative batch of resin-coated cells 10×10 mm^2, which will be presented further in Figure 3, and mechanical tests were performed (i.e., 100 thermal cycles −20 °C +60 °C and 3 cycles UV exposure 20 min each).

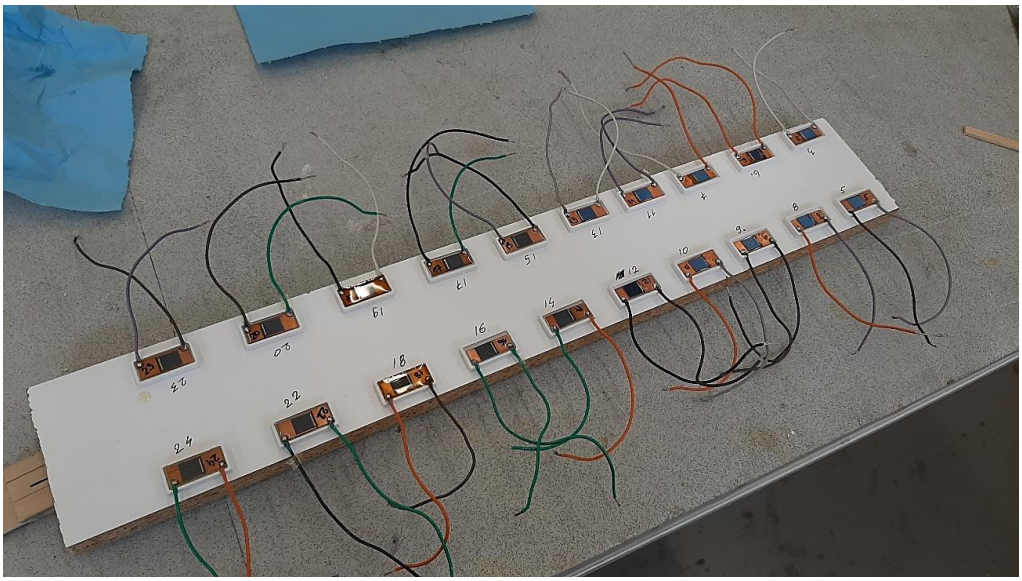


Figure 3. Molds for ensuring the uniformity of coating and the cells coated.

In order to establish which epoxy resin would be suitable for use for the main parameters (open circuit voltage (Voc (mV)) and short circuit current (Isc (mA))) of the photovoltaic cells, photovoltaic cells that were covered with 8 different types of epoxy resins were measured before and after the mechano-climatic tests, and the results are pre-

sented in Table 1. As one can notice, the PV cells show good stability, even after 100 thermal cycles from −20 °C to +60 °C as well as after combined mechano-climatic temperature–UV radiation testing.

Table 1. Main parameters of the photovoltaic cells measured before and after the mechano-climatic tests. Legend: 100 thermal cycles −20 °C to +60 °C and 3 cycles UV exposure 20 min each: c—number of cycles, T—temperature exposure, UV—ultraviolet exposure. Based on the mechanical and optical properties, the epoxy resin that was selected was HT 2, (produced by R&G Faserverbundwerkstoffe GmbH, 71111 Waldenbuch, Germany).

Nr. CS	**without Resin Coverage**		**With Resin Coverage**				
			Type of Resin	**100 Cycles (c) −20 °C + 60 °C**		**UV 3 Cycles of 20 min/c**	
	V_{oc} (mV)	I_{sc} (mA)		V_{oc} (mV)	I_{sc} (mA)	V_{oc} (mV)	I_{sc} (mA)
1	430	4.5	HT2	422	4.5	422	4.30
2	450	4.4	HP E40D	440	3.87	443	3.51
3	450	4.95	HP E65 L	480	5	456	4.59
4	450	4.68	HP E120 WSM-315	458	4.3	452	3.75
5	430	4.96	HP E45 KL	443	4.2	439	3.75
6	410	4.23	HP E25 DM	432	3.56	437	3.20
7	453	5.3	SIKA BIRESIN CR122	440	4.5	472	3.98
8	430	4.84	HP E25 DM	440	4.3	448	3.72
9	450	5	HT2	456	4.8	461	4.18
10	434	5	EP 210	441	4.2	447	3.77
11	450	4.7	HP E120 WSM-315	472	4.7	462	4.30
12	470	5.2	HP E60 K	456	4.6	470	4.21

2.1. Technology Used for Photovoltaic Cells Fabrication

The manufacturing technology that was used for the PV cell structures included four levels of masking: mask M1, which was used to obtain the textured surface of the structure, mask M2, which was used to obtain an active area n+ diffusion, mask M3, which was used for pre–contact/collection electrodes, and mask M4, which was used for the metal contacts. The overlap of these masks was controlled using a group of alignment signs that were located on the diagonal of the plate at a distance of 5 cm to the primary alignment cross. An image of the silica wafer with the photovoltaic cells before separation is presented in Figure 4.

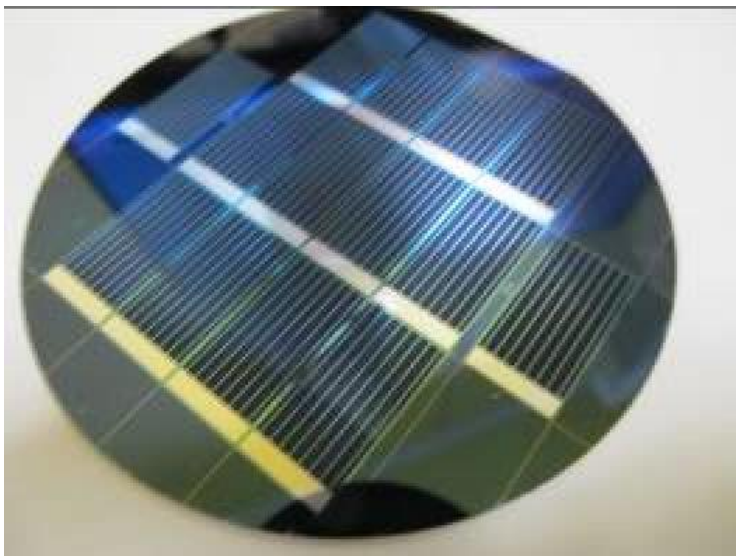


Figure 4. The silica wafer with photovoltaic cells before separation.

The micro-texturing of the active surface in order to reduce the reflection losses at the radiation incident surface was performed by a photolithographic process through the oxide mask realised after the diffusion of boron. An image of the pyramids obtained on the surface of photovoltaic cells is presented in Figure 5.

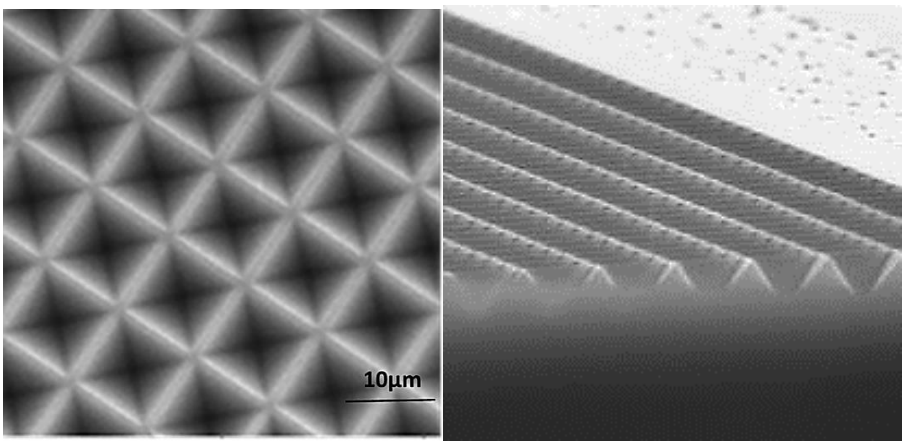


Figure 5. Optical microscope images of micro-texturized surface of photovoltaic cells (pyramids).

Technological process of photovoltaic cell fabrication is presented in Figure 6.

The classic wing manufacturing technology that has been used so far does not allow for the integration of photovoltaic cells, which there is a high probability of during vacuuming due to the pressure exerted on the photovoltaic cells, causing them to exceed the maximum allowable deformation on the areas where the curvature of the wing is greater than 0.5 mm. Following the research and studies that have previously been performed, the necessary changes in the technological process were determined in order to ensure the integration of the cells in the wing without destroying them.

The wing lamination would be conducted in two distinct stages:

a. Embedding the cells in resin support;
b. Lamination of the resistance structure (carbon fibber in resin support).

For this, a technology that allows the incorporation of photovoltaic cells in the protective resin layer that covers the outer surface of the wing was developed, and it is presented in Figure 7.

In the first step of the rolling process, the photovoltaic cells are incorporated in the epoxy resin, eliminating the excess resin, in order to obtain a structure with a minimum thickness and a minimum weight. For this, a technological process similar to "resin infusion" was used, in which resin is introduced through the lower part of the mould, and the surplus is extracted on the edges (flight board and wing attack board) using a perforated extraction tube. The cells represent the first layer followed by a layer of perforated foil, which plays the role of letting the excess resin come out. This is followed by a layer of hard foil that is smaller than the perforated foil, which has a double role: to channel the resin to the upper extraction areas and to ensure a flat surface (the hard material prevents copying of irregularities of cells and electrical connections) on which a layer of the composite material can be applied. This film has the role of protecting the separation plane of the mold and is removed before rolling the resistance structure. The next layer is made of an absorbent material that ensures the vacuum distribution over the entire surface of the wing and collects and channels the excess resin to the exhaust pipe. The vacuum is applied through this pipe, and a buffer tank is also provided to collect the excess rain. The last layer is used for insulation and covers the entire wing.

After the resin has hardened, the technological layers are removed, and the manufacture of the wing is continued by laminating the resistance structure over the resin layer and photovoltaic cells.

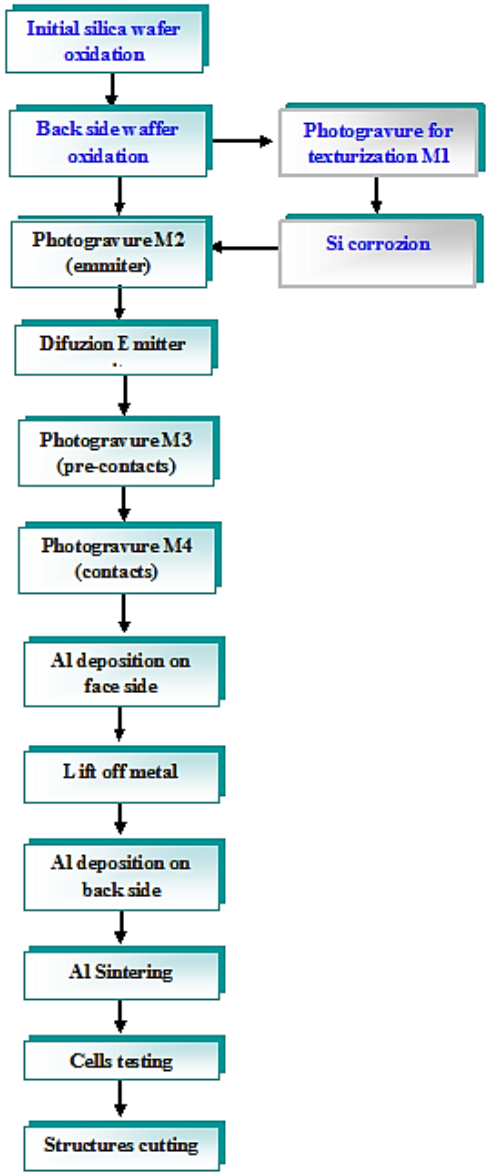


Figure 6. Technological process of photovoltaic cells manufacturing.

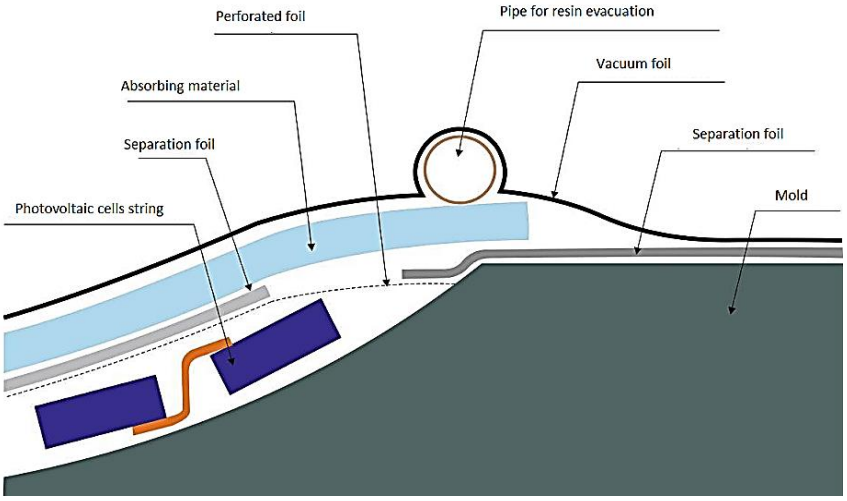


Figure 7. Technology for ultra-light wing with embedded photovoltaic cells fabrication.

2.2. Wing Production and Results

Based on the developed technology, over 3000 micro-structured photovoltaic cells were produced and characterised.

The first step during wing production was to connect the cells in the strings and rows in parallel, as presented in Figure 8, and to produce the first layer of the wing.



Figure 8. The matrix of photovoltaic cells and the mould where will be installed.

After the wing fabrication process, the mould is removed, and the upper side of the wing is ready, with the cells embedded into the epoxy resin, as presented in Figure 9.

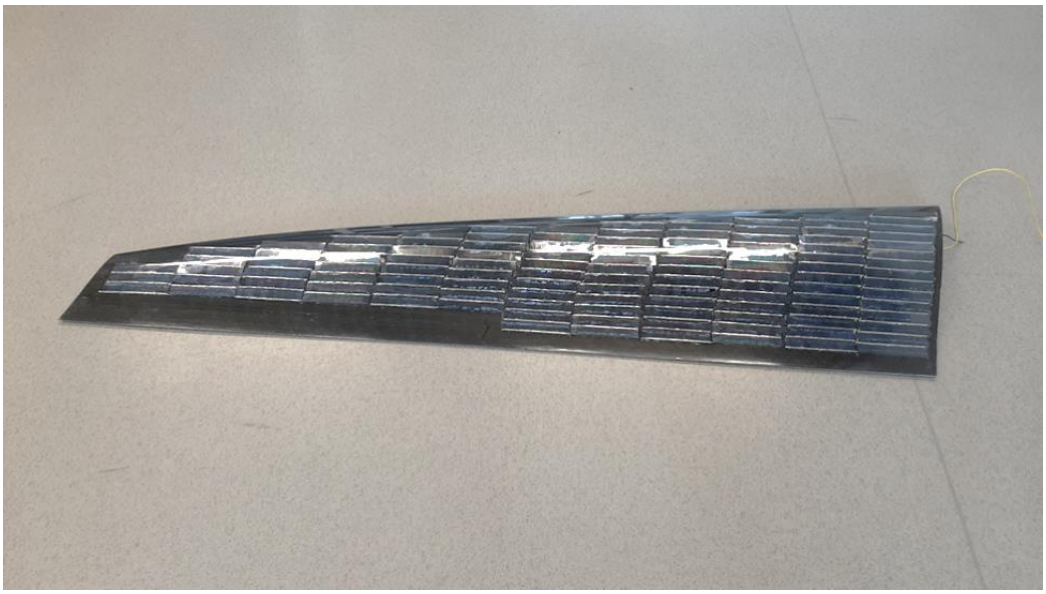


Figure 9. Ultra-light wings with embedded micro-texturized photovoltaic cells.

In order to conduct the required mechano-climatic tests for the produced structure, two small-sized demonstrators were produced, as presented in Figure 10.

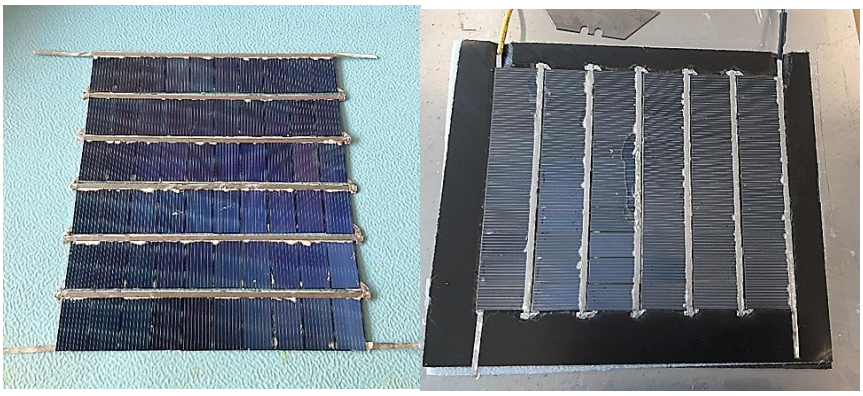


Figure 10. Small-sized demonstrators produced for mechano-climatic testing.

3. Tests and Validation of the Prototype

The equipment used for testing the procedures was an Angelantoni climatic chamber, and a Tira S55240/LS (Cimacolle, 464-06056 Massa Martana (PG)–Italy) vibration tests stand was also used. Pictures of the equipment are presented in Figure 11.



Figure 11. Angelantoni climatic chamber with Tira S55240/LS vibration test stand and demonstrator installed on the shaker table.

Tests Conducted

The tests were conducted based on 6AA-TE 100535 si PM–LEM-10 Ed 8 Rev 3 Standards at a temperature of 25 °C and at RH 37%.

The parameters established for vibrations were:

Sine Sweep: continuous 1 g from 10 HZ to 2 KHz.

Random Vibrations:

-20 Hz to 80 Hz +3 dB/octave, rise to 0.04 g/Hz;

-80 Hz to 350 Hz at 0.04 g/Hz;

-350 Hz to 2 kHz −3 dB/octave, roll off.

The results of the experiments are presented in Figure 12.

As one can see from Figure 12, the random vibration test was conducted, and no typically encountered resonances occurred when the layers of the materials were segregating.

The second batch of tests was conducted to verify the effect of controlled bending on the photovoltaic cells using the Mecmesin 2.5, as presented in Figure 13.

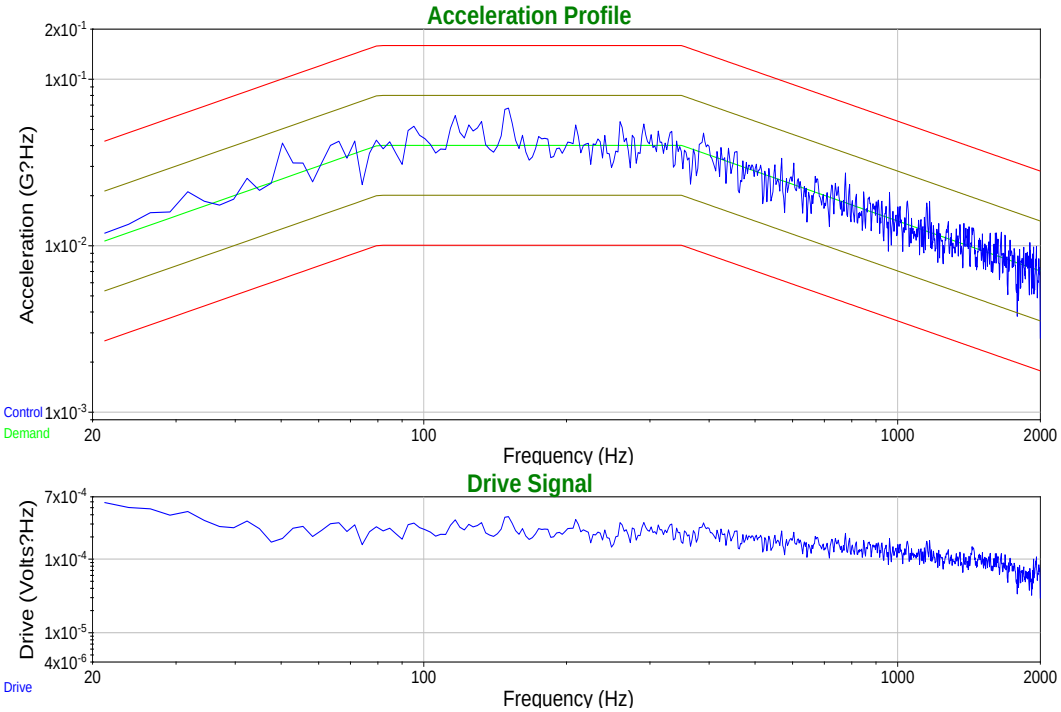


Figure 12. The profile of the random vibration used for testing.



Figure 13. *Cont.*

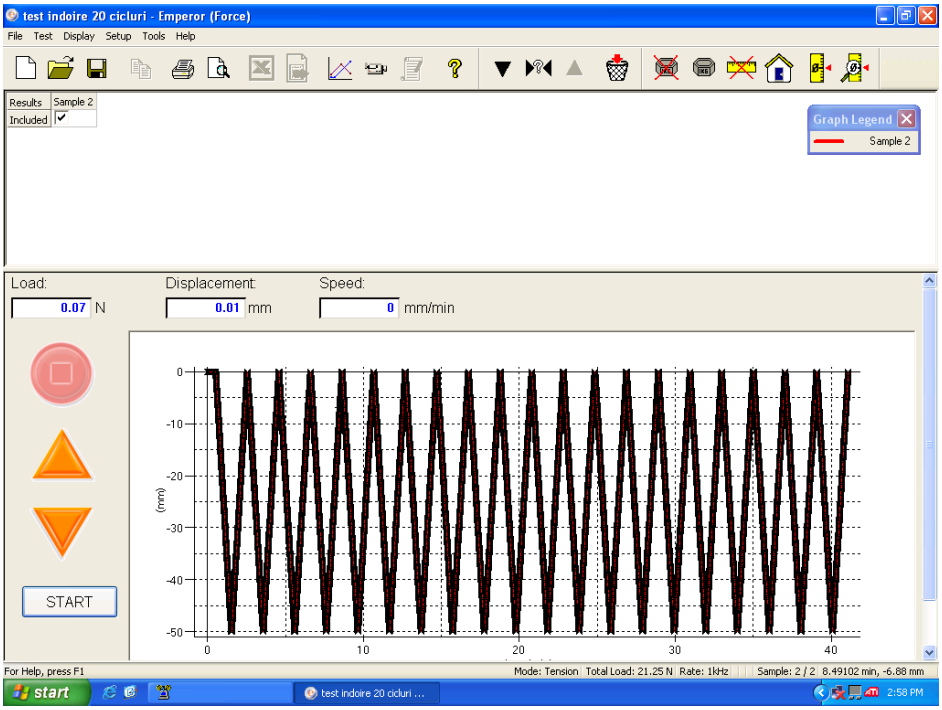


Figure 13. Mecmesin 2.5 I and image of the 20 recorded bending cycles.

This test was dedicated to the study of behaviour at repeated bending. The cycling program was set with the following parameters: minimum displacement = 0, maximum displacement = 2 mm, speed of displacement = 1 mm/min, and landing time = 0.1 min (this would correspond to a wing arrow of 2.2 cm). A total of 20 bending cycles were performed for the test modules.

The new photovoltaic wing was successfully integrated into an UAV prototype for flight trials. Figure 14 shows a photo of this UAV prototype.



Figure 14. Photo of the UAV prototype.

The field testing of the prototype UAV with only one photovoltaic wing showed a 33% improvement in the flight time, which is much larger than the one predicted by the ground

tests (25%). A short video of the prototype flight is presented in Supplementary Material Video S1.

4. Conclusions

By using new composite materials, the newly produced wing had a total weight of 875 g, exceeding the initial design by 25 only grams, which was mainly due to the cell soldering technology, the process of which was conducted manually instead of being automated. The new fabricated wing has the required mechanical flying capabilities since it passed the tests, and the photovoltaic cells embedded in its structure were not damaged due to mechanical factors (bending, vibrations). Experiments that were conducted on the ground provided encouraging results, and it was expected to achieve a 25% increase in the time of flight for the new UAV. Field testing of the prototype UAV with only one photovoltaic wing showed a 33% improvement in the time of flight, which was much larger than the one predicted by the ground tests. The work on adding the second photovoltaic wing is ongoing, and it is expected to lead to increase in the independent flight time of UAVs by more than 60%. A short video of the prototype flight is presented in Supplementary Material Video S1. The fact that the UAV was able to take off, fly for 3.5 h, and land (with parachute), with no damages observed on the wing prove the successful fabrication through the integration of the PVs and that the mechanical tests were adequate. However, for mass production, these tests are not enough, and further developments are required.

5. Patents

This work resulted in patent application No. A100225/06.5.2021 O.S.I.M. Romania.

Supplementary Materials: The following are available online at https://www.mdpi.com/article/10.3390/app112210890/s1, Video S1: Demo flight of the prototype UAV.

Author Contributions: Data curation, O.N.I., M.P.S. and G.I.; formal analysis, O.N.I.; E.M., C.P. and G.I.; funding acquisition, investigation, E.M., O.N.I. and A.I.; methodology, O.N.I., E.M., C.P. and A.I.; project administration, O.N.I.; resources, I.C., O.N.I. and A.I.; supervision O.N.I.; validation, O.N.I., G.I., A.I. and M.P.S.; visualization, and M.P.S.; writing—original draft, O.N.I., G.I. and M.P.S.; writing—review and editing, O.N.I., G.I. and M.P.S. All authors have read and agreed to the published version of the manuscript.

Funding: This work was supported within the framework of the TGE-PLAT project, No. 77/2016, co-financed by European structural funds—POC/2014-2020.

Institutional Review Board Statement: Not applicable.

Informed Consent Statement: Not applicable.

Data Availability Statement: The raw and processed data required to reproduce these findings cannot be shared at this time due to technical or time limitations. The raw and processed data will be provided upon reasonable request to anyone interested anytime until the technical problems are solved.

Acknowledgments: UAV production was entirely supported by SC Autonomous Flight Technology, (Traian Str, No. 152 C, 2nd district, 24042, Bucharest, Romania). Many thanks are also extended to M. Purica from IMT Bucharest for helping with the I-V measurements of the PV cells.

Conflicts of Interest: The authors declare that they have no known competing financial interests or personal relationships that could have appeared to influence the work reported in this paper.

References

1. *Unmanned Aerial Vehicle (UAV) Market Worth $45.8 Billion by 2025-Exclusive Report by MarketsandMarkets™-Bloomberg*; Bloomberg: New York, NY, USA. Available online: https://www.bloomberg.com/press-releases/2019-10-29/unmanned-aerial-vehicle-uav-market-worth-45-8-billion-by-2025-exclusive-report-by-marketsandmarkets (accessed on 1 November 2021).
2. Chu, Y.; Ho, C.; Lee, Y.; Li, B. Development of a solar-powered unmanned aerial vehicle for extended flight endurance. *Drones* **2021**, *5*, 44. [CrossRef]

3. Ridwana, I.; Alfindo, B. The effect of use of solar panels on micro scale fixed-wing UAV type as a power recharging system. *AIP Conf. Proc.* **2019**, *2180*, 020044. [CrossRef]
4. Naidu, Y.; Adali, S. Design and optimization of a medium altitude long endurance UAV wing box structure. *R D J. S. Afr. Inst. Mech. Eng.* **2014**, *30*, 22–29.
5. Green, M.A.; Emery, K.; Hishikawa, Y.; Warta, W.; Dunlop, E.D. Solar cell efficiency tables (Version 45). *Prog. Photovolt. Res. Appl.* **2015**, *23*, 1–9. [CrossRef]
6. Virginia Semiconductor, Inc. Basic Mechanical and Thermal Properties of Silicon. Available online: www.vriginiasemi.com (accessed on 1 November 2021).
7. Ritchie, R.O. Failure of Silicon: Crack Formation and Propagation. In Proceedings of the 13th Workshop on Crystalline Solar Cell Materials and Processes, Vail, CO, USA, 10–13 August 2003.
8. Yablonovitch, E. Statistical ray optics. *J. Opt. Soc. Am.* **1982**, *72*, 899–907. [CrossRef]